Passive Wireless Channel Estimation in RF Tag Network

Yasha Karimi*, Yuanfei Huang*, Akshay Athalye*, Samir Das[†], Petar Djurić* and Milutin Stanaćević*

*Department of Electrical and Computer Engineering, Stony Brook University, Stony Brook, NY 11794

†Department of Computer Science, Stony Brook University, Stony Brook, NY 11794

Email: milutin.stanacevic@stonybrook.edu

Abstract—We envision a future where every object in our living and working environment will carry one or more RF tags. Based on the backscattering tag-to-tag communication link, these RF tags will be connected in a network without the need for the central interrogating device. We present a novel tag architecture that enables estimation of the parameters of wireless tag-to-tag channel by a passive receiver. Sampling the received baseband signal at different reflecting phases at the backscattering tag enables estimation of amplitude and phase of the tag-to-tag channel. The low-power implementation of the channel estimator, after envelope detection, integrates amplification and filtering of the baseband signal that is followed by analog-to-digital conversion. The channel estimator, implemented in 65 nm CMOS technology, has sensitivity of -45 dBm at 2.5% modulation index and consumes 122 nW.

I. Introduction

It is not hard to imagine a future smart home, hospital or elderly care room in which most of the physical objects have attached Radio Frequency IDentification(RFID) tag that enables identification, localization and tracking of the object. Moving forward with this application, the major drawback presents the cost of the supporting infrastructure, namely the number of costly RFID readers. Recently, tag-to-tag communication based on backscattering of ambient RF energy or RF continuous wave signal from a dedicated exciter has been established as an enabling technology for eliminating RFID readers from a network of RF tags [1], [2], [3]. As the tags are tiny, inexpensive and passive and communicate directly with each other without a centralized active reader, they can be truly pervasive and the network of tag can become a part of the physical environment without requiring any additional infrastructure to operate. The excitation signal required for backscattering can either be provided by an intentionally deployed, un-coordinated, zero-intelligence exciter or by ambient RF signal sources such as WiFi APs and TV towers [4], [5],

Wireless channel estimation has been used for enhancing the performance of the communication link [7], [8]. Recently, more emphases in the application of the wireless channel estimation has been on sensing of the surrounding environment. Any movement of living beings or physical objects in the vicinity of the wireless link changes the link parameters due to the change in the reflections of the RF signal. Several 'device-free' activity recognition techniques for inferring activities via analysis of RF signals reflected from objects

and living beings in the surrounding environment have been proposed [9], [10]. These activity recognition techniques use active wireless receivers and perform channel estimation using the well-known IQ demodulation to measure amplitude and phase of the reflected signal [11]. However, these receivers have high power consumption on the order of 1 mW at the minimum [12], [13], [14], which is prohibitive in most RF-powered devices. Prior attempts to achieve a network of passive RF tags with activity recognition required a presence of RFID reader, that exclusively measured the amplitude and phase of signals from each tag (point-to-multipoint) in order to perform RF fingerprinting [15], [16], [17], [18]. The high cost, low scalability and low precision (granularity) of such systems is a blocker to their widespread practical use.

We explore the channel estimation in a passive tag-to-tag link, in which due to limit on the power consumption of the tag, tag can not perform I-Q demodulation. We empower the passive tags with the unprecedented ability to estimate the RF parameters of the wireless channel between pairs of communicating tags. With such capability, the network of RF tags can provide a real-time, precise, fine-grained RF finger-print of the environment. As the tags continuously sense the parameters of the RF channel (amplitude and phase) between neighboring tags, they can detect and classify activities in their environment [19].

The paper is organized as following. In Section II, the passive wireless channel estimation technique is presented. The Section III presents the circuit implementation of the receiving tag that is capable of performing channel estimation. Simulation results are in IV and the concluding remarks are in Section V.

II. PASSIVE CHANNEL ESTIMATION

The foundation of the backscattering communication is the passive transmission achieved by the varying the terminating impedance in the antenna circuit of the transmitting device, as seen in RFID systems in tag-to-reader communication link [20], [21], [22]. The tag typically switches between two terminating impedances, which modulates the reflected signal. As illustrated in Figure 1(a), the backscatter signal has a low modulation index that is resolved by computationally powerful RFID reader. In reader-to-tag link the modulated RF signal received by the tag has a high modulation index and is demodulated by envelope detector.

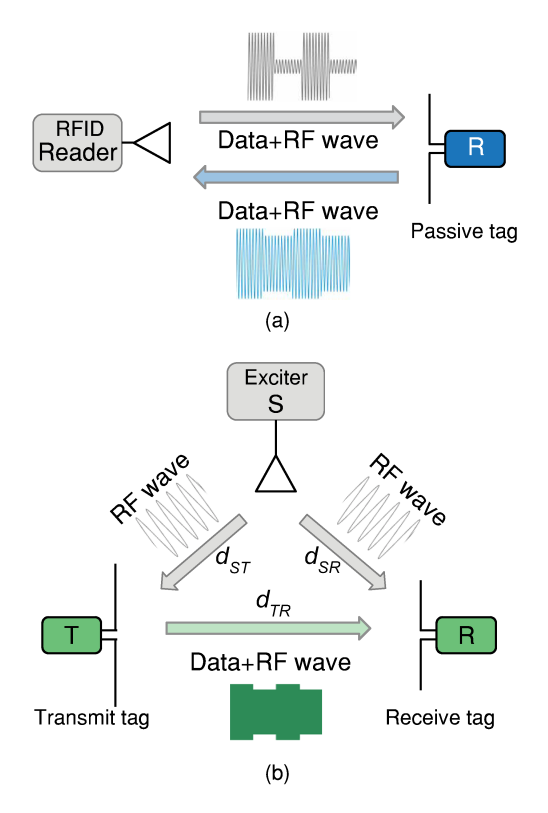


Fig. 1. (a) Communication link in RFID system. (b) Backscatter tag-to-tag communication link.

To eliminate RFID reader from the system and transform a central-based system to a distributed system, the tags, with the circuit architecture similar to RFID tags, should be able to communicate in the presence of excitation RF signal. In a tag-to-tag link, a transmitting(Tx) tag modulates the reflecting signal in the same fashion as in tag-to-reader link and the backscattered signal with low modulation index is resolved by a receiving(Rx) tag with the passive envelope detector as demodulator [23], as illustrated in Figure 1(b). As the sensitivity of the envelope detector used in a conventional RFID tag is significantly lower than the sensitivity of the active receiver in RFID reader, the range of tag-to-tag link becomes limited. However, by advancing the design of the demodulator under limited power budget, the link range can be extended to few meters [23].

To demonstrate how the wireless tag-to-tag channel can be passively estimated, we first express the envelope of the RF signal at the Rx tag as a function of the reflecting phase of the Tx tag [19]. The incident signals at the Rx tag in tag-to-tag link are illustrated in Figure 2, assuming that presence of dedicated exciter that provides continuous wave(CW) signal. When the antenna circuit in Tx tag is open, Rx tag only receives the signal from the exciter

$$v_{R1}(t) = A_E(t)e^{j(\omega t + \theta_E(t))}, \tag{1}$$

where v_{R1} is the signal received at the Rx tag. A_E and θ_E are the amplitude and the phase of the received signal and are dependent on the reflections from the environment. When Tx

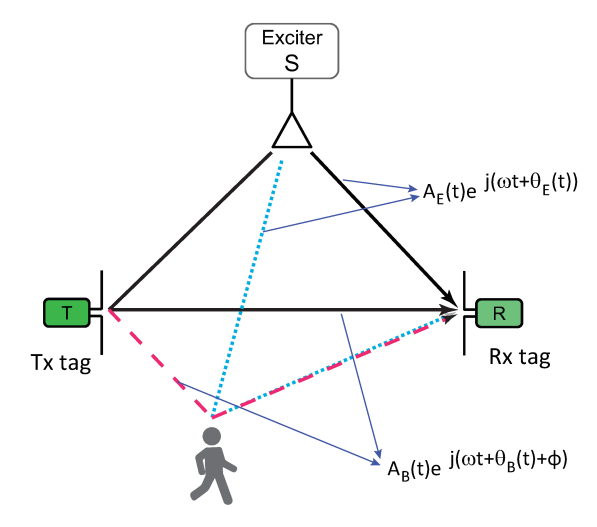


Fig. 2. The direct and reflected signals in backscattering tag-to-tag link scenario with a person present in the vicinity.

tag reflects the incident RF signal with the phase change ϕ , the reflected signal is superimposed on the exciter signal

$$v_{R2}(t) = A_E(t)e^{j(\omega t + \theta_E(t))} + A_B(t)e^{j(\omega t + \theta_B(t) + \phi)},$$
 (2)

where A_B is the amplitude of the backscatter and θ_B is the phase of the *exciter-Tx-Rx* channel in the received signal. We define the baseband signal, obtained by envelope detection, as the difference between the amplitude of RF signals v_{R2} and v_{R1} at Rx tag. The difference between two amplitudes simplifies to:

$$\Delta v_R(t) = v_{R2}^{amp}(t) - v_{R1}^{amp}(t)$$

$$\approx A_B \cos(\phi + \theta_B(t) - \theta_E(t)).$$
(3)

when the amplitude of the backscatter signal A_B is much smaller than the amplitude of the excitation signal A_E . We denote the phase difference between the *exciter-Rx* and *exciter-Tx-Rx* wireless channels as $\theta_{BC}(t) = \theta_B(t) - \theta_E(t)$, and call it *backscatter channel phase*. The amplitude and phase A_B and $\theta_{BC}(t)$ define the backscatter tag-to-tag channel.

The wireless channel estimation through measurement of the amplitude and phase of the channel enables sensing of the changes in the surrounding environment. On a passive tag, we can measure only the amplitude difference Δv_R for a reflection phase ϕ and not the amplitude and phase of the channel. However, if Δv_R is measured for a set of the deterministic reflection phases ϕ in a 0 to π range, both the amplitude and phase A_B and $\theta_{BC}(t)$ can be obtained [19]. The accuracy of the amplitude and phase measurement depends on the selected number of reflection phases at the Tx tag.

III. CIRCUIT IMPLEMENTATION

In backscattering tag-to-tag link, the channel estimation is performed by multiphase probing as described in Section II. The modulator of Tx tag switches between a set of terminating impedances that represent different reflecting phases. Channel estimator of Rx tag measures the baseband signal Δv_R at each

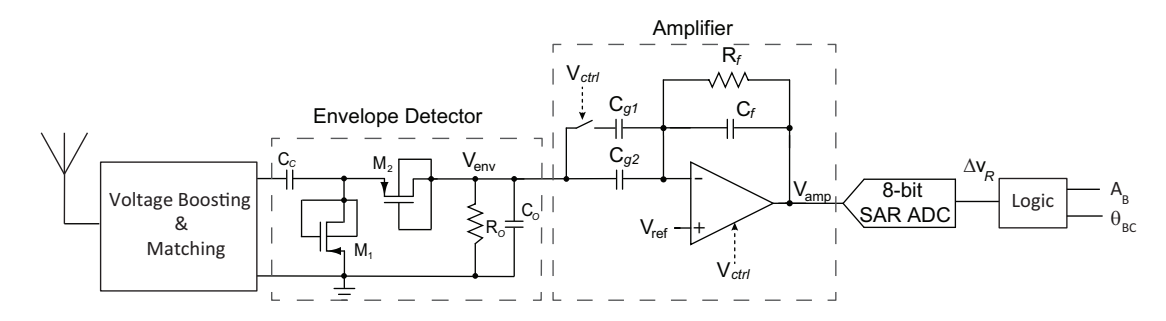


Fig. 3. Architecture and circuit implementation of the passive tag-to-tag channel estimator.

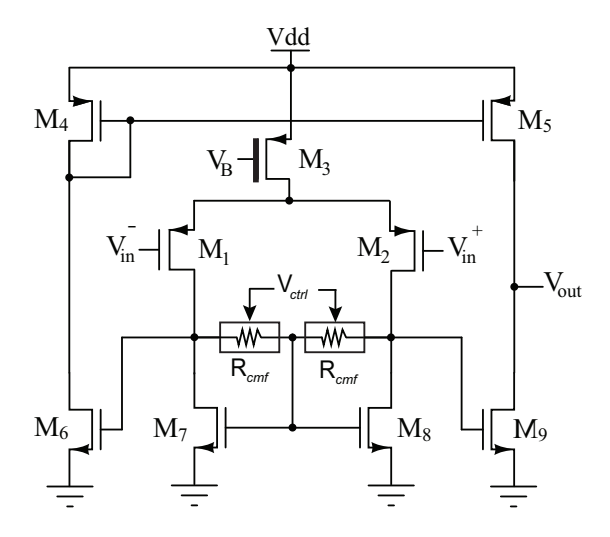


Fig. 4. Schematic of the class A operational amplifier.

reflecting phase in order to compute amplitude A_B and phase θ_{BC} of tag-to-tag channel. The quantification of the baseband signal is challenging due to the low modulation index of the received RF signal and low sensitivity of envelope detector, as well as wide range of the possible input RF powers and modulation indexes. Additionally, the power budget for the channel estimator is on the order of 100s nW, if the RF tag is to operate with the targeted input RF power of -25 dBm. The block diagram of the proposed implementation of the channel estimator is shown in Figure 3.

A. Matching, Voltage Boosting and Envelope Detector

For extraction of the envelope of the received RF signal, a voltage doubler is used. To increase the sensitivity of the passive rectifier, we applied voltage boosting and matching between antenna and the rectifier enlarging voltage difference at the input of the rectifier [24], [25]. The sizing of the transistors and low-pass filter is optimized in terms of the output voltage amplitude and ripple voltage.

B. Amplifier Design

Due to the inherent low modulation index of RF received signal in tag-to-tag link, the baseband signal V_{env} presents a small variation on top of a large pedestal signal. We employ architecture with integrated high-pass filtering and

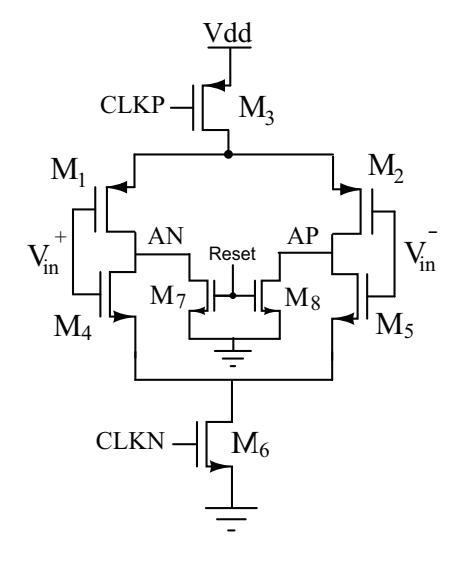


Fig. 5. Schematic of the SAR ADC comparator.

amplification to resolve this signal. Due to large variation in the input power and modulation index of the input RF signal, the gain of the amplifier can be selected as 1 or 6. Class A operational amplifier is used and it is shown in Figure 4. Transistors with standard threshold voltage are employed so that the moderate-inversion biasing is possible, except for transistor M_3 . M_3 is chosen as a high threshold transistor in order to reduce the leakage current. To increase the open-loop gain, input transistors are biased in the weak-inversion mode, while the other transistors are operating in the moderate or strong inversion for better linearity and lower noise. Resistors R_{cmf} provide enhanced stability to the amplifier by fixing the gate voltage of transistors M_6 and M_9 . R_{cmf} values can be controlled by V_{ctrl} in order to change bandwidth of amplifier and reduce the closed-loop gain to unity in case of a higher amplitude of the signal at the output of envelope detector. The capacitances C_{g1} , C_{g2} and C_f are set to 5 pF, 1 pF, and 1 pF, respectively. Resistor R_f is implemented a high-resistive diode-connected transistor.

C. SAR ADC Design

For quantization of the baseband signal, 8-bit successive approximation(SAR) ADC with sampling rate of 40 kS/s was implemented [26]. For achieving high power efficiency, the

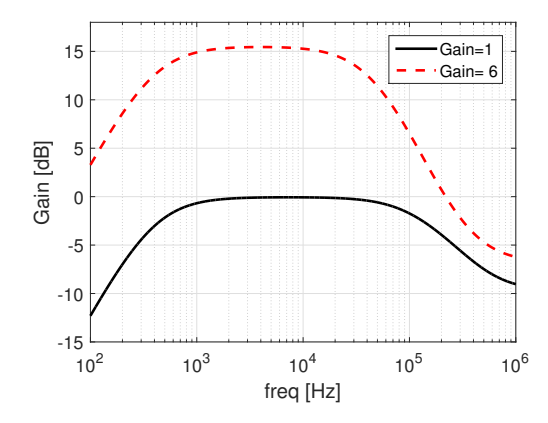


Fig. 6. Transfer function of the amplifier with integrated high-pass filter with two possible closed-loop gains.

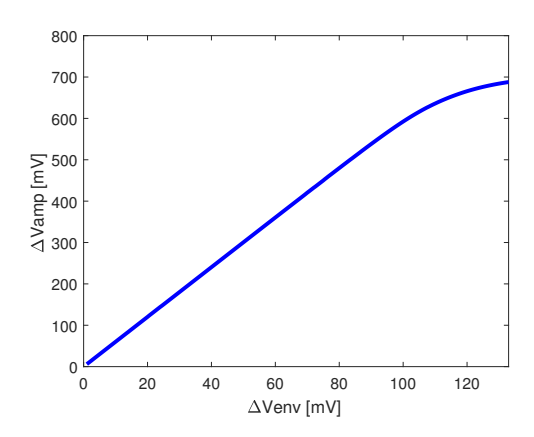


Fig. 7. Output of the amplifier as a function of the amplitude of the baseband signal after the envelope detector.

unit capacitors are customized to 0.5 fF and asynchronous dynamic logic technique is use in design of SAR logic. A duty-cycled reference generation and a bi-directional dynamic comparator lower the noise and power consumption. The designed comparator is shown in Figure 5 where AP and AN are connected to a latch comparator. With 8.3 kHz input sinewave signal, ADC achieves ENOB of 8.04 and consumes 72 nW at 0.8 V voltage supply. The ADC occupies area of 95 μ m x 64 μ m.

IV. SIMULATION RESULTS

The channel estimator is designed in 65 nm CMOS technology with the supply voltage of 0.8 V. The simulations are performed on extracted layout.

The transfer function of the amplifier with integrated highpass filter for two closed-loop gain settings is depicted in Figure 6. The output voltage of the amplifier as a function of the voltage after the envelope detection is shown in Figure 7 demonstrating high linearity up to 80 mV at the input of the amplifier when the closed-loop gain is set to 6.

To demonstrate the performance of the overall analog frontend shown in Figure 3, the input power was held at -45 dBm

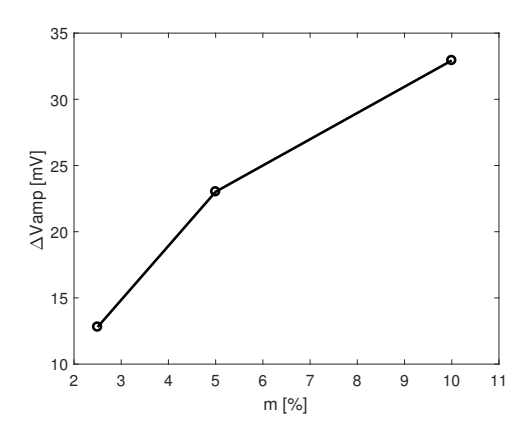


Fig. 8. Amplifier output for different input modulation index with the input power at the antenna of $P_{in}=$ -45 dBm.

TABLE I PERFORMANCE SUMMARY OF RF TAG CHANNEL ESTIMATOR

Parameter	Value
Technology	65 nm
Supply Voltage	0.8 V
Total Power consumption	122~nW
Total Input Ref Noise	94 μV_{rms}
Carrier Frequency	900MHz
Data Rate	4 kHz
Sensitivity*	-45 dBm

*at 2.5% modulation index

and signal with different ASK modulation index at data rate of 4 Kbps was applied. The input power of -45 dBm represents the sensitivity of the channel estimator. The output of the amplifier as a function of the modulation index is shown in Figure 8. Total power consumption of the channel estimator is 122 nW which makes it suitable for an ultra lower power system. Summary of the performance of the proposed channel estimator is outlined in Table I.

V. CONCLUSION

We presented the implementation of the wireless channel estimation in tag-to-tag link. RF tags embedded in a typical living space, empowered with this novel form of passive RF sensing, will be able to sense activities and interactions among various entities around them, both tagged and not-tagged. This enables applications such as fine grain tracking of human movements, activity and gesture recognition and human-object interactions. These capabilities in turn will provide an ability to query and reason about the environment in order to infer a wide range of analytic information. All this will be achieved without the occupants (humans) within the environment having to carry or wear any devices (device free).

ACKNOWLEDGMENT

This research was supported by the National Science Foundation under grant number CNS-1763843.

REFERENCES

- [1] M. Hessar, A. Najafi, and S. Gollakota, "Netscatter: Enabling large-scale backscatter networks," *arXiv preprint arXiv:1808.05195*, 2018.
- [2] K. Han and K. Huang, "Wirelessly powered backscatter communication networks: Modeling, coverage, and capacity," *IEEE Transactions on Wireless Communications*, vol. 16, no. 4, pp. 2548–2561, 2017.
- [3] J. Ryoo, J. Jian, A. Athalye, S. R. Das, and M. Stanaćević, "Design and evaluation of bttn: A backscattering tag-to-tag network," *IEEE Internet* of Things Journal, 2018.
- [4] V. Liu, A. Parks, V. Talla, S. Gollakota, D. Wetherall, and J. R. Smith, "Ambient backscatter: wireless communication out of thin air," in ACM SIGCOMM Computer Communication Review, vol. 43, no. 4. ACM, 2013, pp. 39–50.
- [5] P. Zhang, D. Bharadia, K. Joshi, and S. Katti, "Hitchhike: Practical backscatter using commodity wifi," in *Proceedings of the 14th ACM Conference on Embedded Network Sensor Systems CD-ROM*. ACM, 2016, pp. 259–271.
- [6] S. Kim, R. Vyas, J. Bito, K. Niotaki, A. Collado, A. Georgiadis, and M. Tentzeris, "Ambient rf energy-harvesting technologies for self-sustainable standalone wireless sensor platforms," *Proceedings of the IEEE*, vol. 102, no. 11, pp. 1649–1666, 2014.
- [7] H. Meyr, M. Moeneclaey, and S. Fechtel, Digital communication receivers: synchronization, channel estimation, and signal processing. John Wiley & Sons, Inc., 1997.
- [8] Y. Li, N. Seshadri, and S. Ariyavisitakul, "Channel estimation for ofdm systems with transmitter diversity in mobile wireless channels," *IEEE Journal on Selected areas in communications*, vol. 17, no. 3, pp. 461–471, 1999.
- [9] S. Sigg, U. Blanke, and G. Troster, "The telepathic phone: Frictionless activity recognition from wifi-rssi," in *Pervasive Computing and Communications (PerCom)*, 2014 IEEE International Conference on. IEEE, 2014, pp. 148–155.
- [10] Q. Pu, S. Gupta, S. Gollakota, and S. Patel, "Whole-home gesture recognition using wireless signals," in *Proceedings of the 19th annual International Conference on Mobile Computing & Networking*. ACM, 2013, pp. 27–38.
- [11] H. Simon and M. Michael, "Modern wireless communications," Publisher: Prentice Hall, 2005.
- [12] J. Blanckenstein, J. Klaue, and H. Karl, "A survey of low-power transceivers and their applications," *IEEE Circuits and Systems Mag*azine, vol. 15, no. 3, pp. 6–17, 2015.
- [13] G. Papotto, F. Carrara, and G. Palmisano, "A 90-nm cmos threshold-compensated rf energy harvester," *IEEE Journal of Solid-State Circuits*, vol. 46, no. 9, pp. 1985–1997, 2011.
- [14] E. R. R.E. Barnett, J. Liu, and S. Lazar, "A rf to dc voltage conversion model for multi-stage rectifiers in uhf rfid transponders," *IEEE Journal* of Solid-State Circuits, vol. 44, no. 2, pp. 354–370, 2009.
- [15] J. Huiting, H. Flisijn, A. B. J. Kokkeler, and G. J. M. Smit, "Exploiting phase measurements of EPC Gen2 RFID tags," in *RFID-Technologies* and Applications (RFID-TA), 2013 IEEE International Conference on. IEEE, 2013, pp. 1–6.
- [16] H. Li, C. Ye, and A. P. Sample, "IDSense: A human object interaction detection system based on passive UHF RFID," in *Proceedings of the* 33rd Annual ACM Conference on Human Factors in Computing Systems, 2015, pp. 2555–2564.
- [17] R. Parada, J. Melià-Seguí, A. Carreras, M. Morenza-Cinos, and R. Pous, "Measuring user-object interactions in IoT spaces," in *RFID Technology* and Applications (RFID-TA), 2015 IEEE International Conference on, 2015, pp. 52–58.
- [18] K. Fishkin, B. Jiang, M. Philipose, and S. Roy, "I sense a disturbance in the force: Unobtrusive detection of interactions with rfid-tagged objects," in *International Conference on Ubiquitous Computing*. Springer, 2004, pp. 268–282.
- [19] J. Ryoo, Y. Karimi, A. Athalye, M. Stanaćević, S. Das, and P. Djurić, "Barnet: Towards activity recognition using passive backscattering tagto-tag network," in *Proceedings of the 16th Annual International Con*ference on Mobile Systems, Applications, and Services. ACM, 2018, pp. 414–427.
- [20] K. Finkenzeller, RFID Handbook: Fundamentals and Applications in Contactless Smart Cards and Identification. New York, NY, USA: John Wiley & Sons, Inc., 2003.

- [21] J. Griffin and G. Durgin, "Complete link budgets for backscatter-radio and rfid systems," *IEEE Trans. on Antennas and Propagation Magazine*, vol. 51, no. 2, pp. 11–25, 2009.
- [22] C. Boyer and S. Roy, "Backscatter communication and rfid: Coding, energy, and mimo analysis," *IEEE Transactions on Communications*, vol. 62, no. 3, pp. 770–785, 2014.
- [23] Y. Karimi, A. Athalye, S. Das, P. Djurić, and M. Stanaćević, "Design of backscatter-based tag-to-tag system," in *IEEE International Conference* on RFID (RFID), 2017.
- [24] H. Jiang, P. P. Wang, L. Gao, P. Sen, Y. Kim, G. M. Rebeiz, D. A. Hall, and P. P. Mercier, "24.5 a 4.5nw wake-up radio with 69dbm sensitivity," in 2017 IEEE International Solid-State Circuits Conference (ISSCC), Feb 2017, pp. 416–417.
- [25] S. Oh and D. D. Wentzloff, "A 32dbm sensitivity rf power harvester in 130nm cmos," in 2012 IEEE Radio Frequency Integrated Circuits Symposium, June 2012, pp. 483–486.
- [26] M. Liu, K. Pelzers, R. van Dommele, A. van Roermund, and P. Harpe, "A106nw 10 b 80 ks/s sar adc with duty-cycled reference generation in 65 nm cmos," *IEEE Journal of Solid-State Circuits*, vol. 51, no. 10, pp. 2435–2445, Oct 2016.